



TRACKING OF RIVER SURFACE FEATURES BY SPACE TIME IMAGING

I. FUJITA^{1,c}, Y. KOSAKA¹, M.HONDA¹, A. YOROZUYA²

¹Department of Civil Engineering, Kobe University, 1-1 Rokkodai, Nada, Kobe 657-8501, Japan

²International Center for Water Hazard and Risk Management, PWRI, 1-6, Minamihara, Tsukuba 305-8515, Japan

^cCorresponding author: Tel.: +81788036439; Fax: +81788036439; Email: ifujita@kobe-u.ac.jp

KEYWORDS:

Main subjects: environment flow, flow visualization, flow measurement

Fluid: river flow, flood flow

Visualization method(s): space time image

Other keywords: water surface feature, STIV, turbulence

ABSTRACT: River surface exhibits various features depending on flow conditions. In a still condition, a water surface is kept flat and reflects the surrounding light like a mirror. With increasing the flow, the water surface begins to exhibit complicated features generated and visualized by turbulence effects. Such water surface features have known to be advected in the downstream direction with the surface flow for a relatively large flow velocity and this property has been used for non-intrusive flow measurements such as imaging or radio wave techniques. However, the properties of such water surface features have not been investigated in detail. In this research, river surface images taken at the time of a flood occurred in the Kinu River in 2011 were examined to obtain a reliable surface velocity distribution by tracking surface features efficiently using a space-time imaging technique proposed by the authors. As a result, the surface velocity measured by the imaging technique was found to be in good agreement with the results measured by radio-wave velocity meter.

INTRODUCTION

The data acquisition of river discharges is indispensable for a proper management of river systems but has a large uncertainty because the conventional measurement method of a flood discharge could yield a significant error depending on the flood condition. The conventional method mainly used in Japan is a float method that uses several floats to measure mean velocities along their paths and integrates them over the cross-sectional area. The float method is considered to be a robust method and applicable to various conditions; however, for a very large flood condition, for which an accurate data acquisition is keenly required to examine the extreme hydrological events, this method sometimes failed to continue because manual operations near the river or from a bridge become extremely dangerous in such a flood condition. Moreover, tracerability of a float to the local mean flow in a significantly turbulent condition is questionable in such a condition. Therefore, alternative methods such as an acoustic Doppler current profiler (ADCP) (Muste et al. 2004, Dinehart and Burau 2005, Oberg and Mueller 2007), a side-looking ADCP (Le Coz et al. 2008), a UHF radar (Teague et al. 2007), a radio-wave velocity meter or imaging techniques have been developed. The first two methods measure the volumetric water movement while the latter three methods measure the surface velocity non-intrusively by assuming that water surface features composed of irregular surface roughness is advected with the surface flow. As for the imaging method, the large-scale particle image velocimetry (LSPIV) (Fujita and Komura 1994, Fujita et al. 1997, Fujita, et al. 1998) and the space-time image velocimetry (STIV) (Fujita et al. 2007) have been developed, with success to obtain surface velocity distributions in many river floods. However, as a comparison with other methods were rarely conducted (Sun et al. 2010), quantitative evaluations of the measurement results were not sufficient. Therefore, in the present research, we conducted simultaneous measurements by using an imaging technique, a radio wave velocity meter and an ADCP at the time of a flood occurred in the Kinu River in 2011. The measurements were continued for about a half day trying to capture the peak discharge of the flood. In the application of the imaging technique, the same water surface was videotaped from two different angles for improving the measurement accuracy.



OUTLINE OF STIV

In applying imaging techniques, the relation between the screen coordinates (x,y) and the physical coordinates (X,Y,Z) has to be established beforehand by using several mark point coordinates. A one-to-one relationship between a point on a water surface (X,Y) and a screen coordinates (x,y) can be obtained with the water level information which is assumed to be horizontal. The relation can be expressed generally as

$$x = F(X,Y), \quad y = G(X,Y) \quad (1,2)$$

or in a reverse form

$$X = f(x,y), \quad Y = g(x,y). \quad (3,4)$$

In the application the space time image velocimetry to surface flow measurements, an image intensity distribution in a search line placed parallel to the streamwise direction. If the main flow is viewed from a right angle, image intensity distribution in the search line can be used directly, but in general the viewing angle is somewhat skewed from the flow

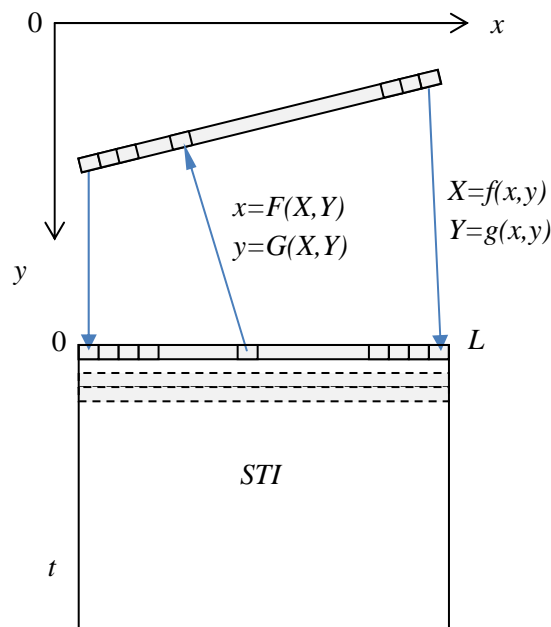


Fig.1 How to construct STI

direction. Therefore, the image intensity distribution has to be obtained with care by considering the above-mentioned mapping relation. Fig.1 shows the method how to construct a space-time image (STI). First, the physical coordinates of the two ends of the search line are calculated by eqs.(3) and (4). L is the physical length of the search line. The physical coordinates along L is divided into the number of pixels equal to that of the search line in the screen coordinates. The image intensity at a point (X,Y) in STI can be obtained by picking up the value at (x,y) calculated from eqs.(1) and (2). As the coordinates calculated by eqs.(1) and (2) do not always be integer values, the image intensity at (x,y) is obtained by a two dimensional interpolation using nearby image data.

Once the STI was constructed, the orientation angles of the image features appeared in the STI can be calculated by the following equation (Fujita et al. 2007),

$$\tan 2\phi = \frac{2J_{xt}}{J_{tt} - J_{xx}} \quad (5)$$

where



$$J_{xx} = \int_A \frac{\partial g}{\partial x} \frac{\partial g}{\partial x} dx dx, \quad J_{xt} = \int_A \frac{\partial g}{\partial x} \frac{\partial g}{\partial t} dx dt, \quad J_{tt} = \int_A \frac{\partial g}{\partial t} \frac{\partial g}{\partial t} dt dt, \quad (6-8)$$

$g(x,t)$: grey level intensity on STI and A is the area of a small segment that divides STI into a number of portions. In calculating the mean value of orientation angle for each small segment, the value of coherency defined by

$$C = \frac{\sqrt{(J_{tt} - J_{xx})^2 + 4J_{xt}^2}}{J_{xx} + J_{tt}} \quad (9)$$

is used as a weighting function. The coherency is a measure of image pattern coherence and takes a value between zero and one; for ideal local orientation the value becomes one and for an isotropic gray image it becomes zero. Therefore, the value of coherency can be used to pick up the orientation angles with more reliable directional information. The mean orientation angle can thus be calculated by the following equation,

$$\bar{\phi} = \int \phi C(\phi) d\phi / \int C(\phi) d\phi. \quad (10)$$

Fig.2 shows an example of orientation angles, coherency distribution and the corresponding histogram of orientation angle. It is obvious that the orientation angle for each small segment yields an angle parallel to the image pattern and the histogram shows a sharp peak. The coherency distribution shows larger (or darker) levels where a clearer pattern appears in the STI.

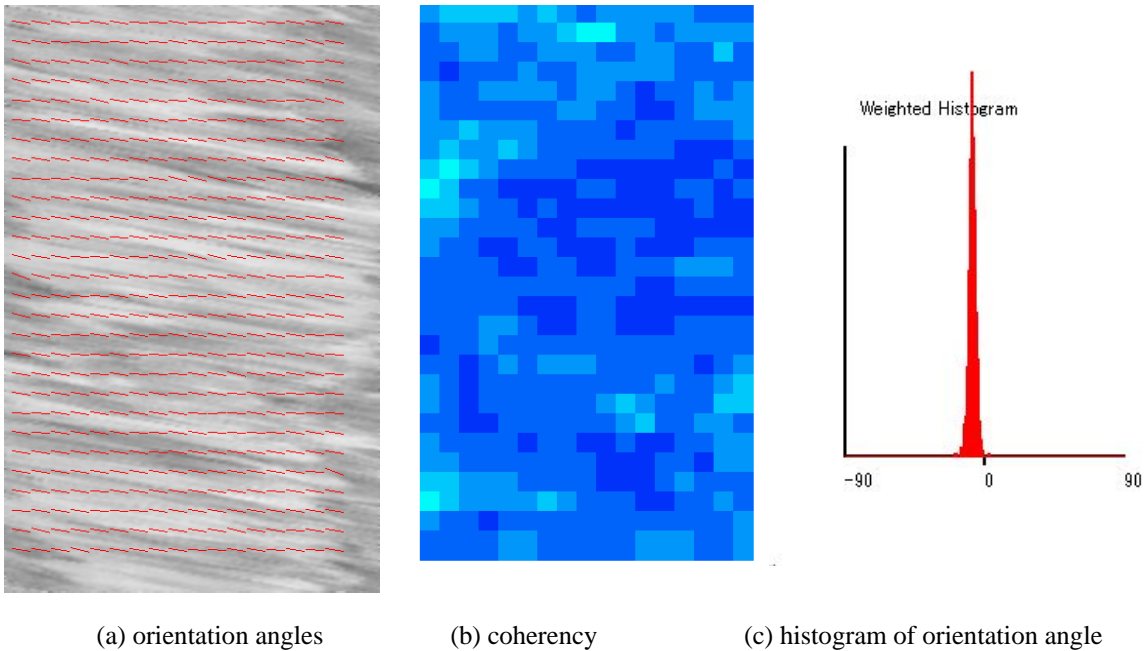


Fig.2 Main procedure of the space-time image velocimetry (STIV); dark color corresponds to larger coherency in (b)

FEATURES OF SPACE TIME IMAGE

As previously mentioned, we conducted river surface flow measurements of the 2011 flood of the Kinu River in Japan. Views from the left and right banks are respectively shown in Fig.3, in which search lines for STIV lying on the same lines, are drawn. The physical length of the search line was set at ten meters. The image size is 1920 by 1080 pixels, which is the size of a high definition image. The video camera from the right bank was set on the bank, while the other camera was installed on the bridge shooting the image from the left bank side. Since the left video camera is positioned at a higher location than the right camera, the spacing between the search lines is a little larger than the left



one. Several boards with a cross mark, whose 3D coordinates were precisely measured, were placed on both sides of the river for obtaining the mapping relations between the screen and the physical coordinates. The water level was

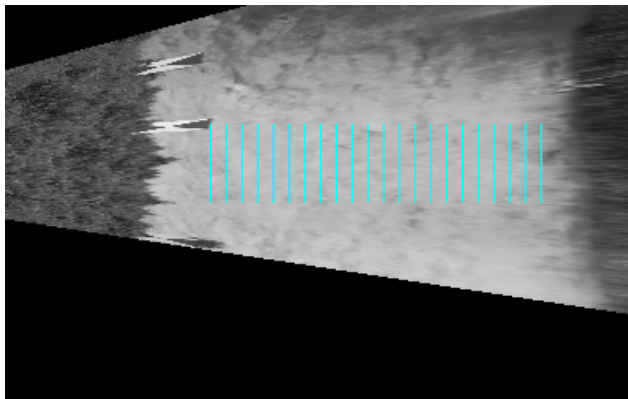


(a) from right bank camera

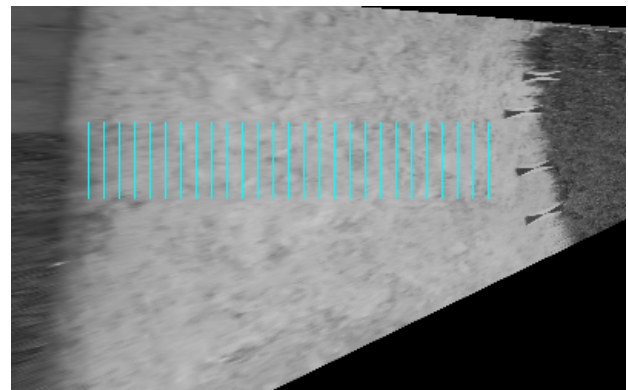


(b) from left bank camera

Fig.3 River surface images of the Kinu River flood and search lines; 11:53:23, Sept.2, 2011



(a) from right bank camera



(b) from left bank camera

Fig.4 Rectified images of the images shown in Fig.3

measured at a gauging station located just upstream of the bridge. Fig.3 shows irregularities of the water surface features generated during flood mainly due to open channel turbulence. The image intensity distributions produced by specular reflections varies with the direction and intensity of the solar insolation. As the weather was cloudy during the measurements, there was no direct solar insolation from the sun; therefore the surface images viewed from both banks displays similar specular reflections. When there is a direct sunlight from the other side of a video camera, the image intensity at some portion of the water surface could be saturated which would make the image analysis difficult; therefore the usage of a pair of video cameras shooting the water surface from different angles, as in the present case, is recommended for obtaining appropriate surface images for river flow measurements in natural conditions. To examine the accuracy of the mapping relations between screen and physical coordinates established in the present study, the oblique angle images shown in Fig.3 are rectified as provided in Fig.4. The images were reconstructed with a basic pixel size of 0.1m. The search lines with a length of ten meters are aligned properly in parallel with an equal spacing of

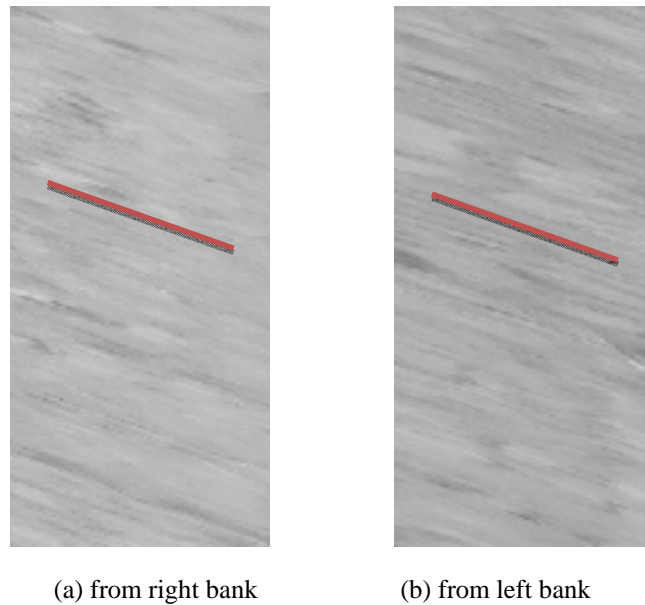


Fig.5 Comparison of STI for the same duration from both video cameras(vertical=20second, horizontal=10m)

two meters. It should be noted that the width of the river surface zone does not always coincides with the actual width because the edge of water in the near side is usually invisible hindered by the front bank. A relatively dark zone in the upper area in Fig.4(a) is due to the shadow of the bridge.



Fig. 6 Surface view at different time; 16:14:27, Sept.3, 2011

In order to examine the traceability of water surface features, space time images (STI) for a search line with the same physical location on the water surface are compared in Fig.5. Fig.5(a) is obtained from the video camera on the right bank and Fig.5(b) is obtained from the other one. The starting time of the vertical time axis of STI is 11:53:23 a.m. on Sept.2 in 2011, which is almost the same for the respective STI. Fig.5 shows that the pattern of surface features does not coincide with each other because the properties of specular reflection differs significantly when veiwed from oposite directions. It should be noted, however, that the orientation angle appeared in each STI is almost the same



despite the difference of image features. The streamwise velocities obtained from these STIs are 3.1m/s from the left videocamera and 3.2m/s from the right video camera, which are almost the same value. To clarify the traceability of such surface features more in detail, several STIs obtained at a time different from Fig.5, i.e. at 4:14:27 pm on Sept.3, indicated respectively in Fig.6 are shown in Fig.7 and Fig.8. The water level rose about 0.97m at this time. The number indicated in the figure corresponds to the location of STI from the left bank shown in Fig.6. The number in the bracket is the velocity obtained by STIV. The spacing between the STIs in Fig.7 and Fig.8 is 4m, therefore the STIs covers the transverse range of 44m of the water zone. Please note the location of No.0 in Fig.7 corresponds to No.5 in Fig.8 because search lines up to No.4 cannot be seen from the left bank. It is obvious that every STI displays clear and almost unidirectional orientation patterns but with slightly different angles in each image, which demonstrates the evidence that

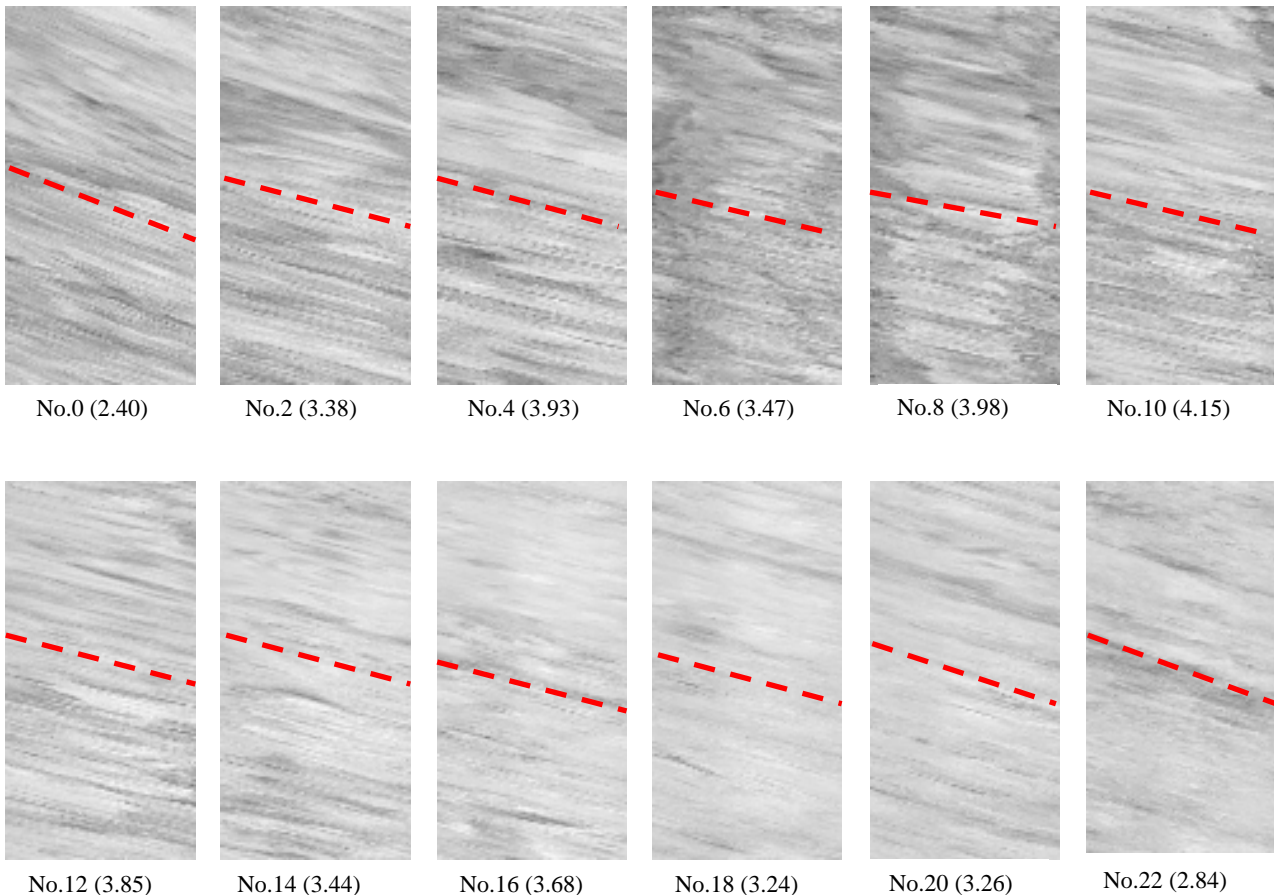


Fig.7 STIs from right bank video camera; horizontal scale is 10m and downward vertical scale is 20 seconds, the number in the bracket is velocity obtained by STIV, the starting time is 4:14:27 pm on Sept.3, 2011

the surface features were advected with the local surface velocity. The velocity value indicated in the figure were obtained from the STIV algorithm. As can be seen from Fig.6, the intensity of specular reflections observed from the two video cameras were significantly different with each other, i.e. the image from the right video camera showed strong reflections from the water surface ripples while the other showed relatively vague pattern. It should be noted that, despite the difference of image features in each STI observed from different angles, the image orientation measured by STIV yielded a similar pattern for each angle, that is similar velocity distributions were obtained by using video images from different angles.

COMPARISON WITH RADIO-WAVE VELOCITY METER



In the present flood flow measurements, a radio-wave velocity meter was installed at the bridge for a local surface flow measurements, in addition to the image capturing devices. This instrument can measure the water surface velocity by tracking the surface irregularities or ripples by utilizing the Dopple effect of radio-wave reflected from a portion of water surface, with a diameter of about one meter. In the present measurement, the measurement location by the radio-wave velocity meter was almost the same area as in STIV measurements. As this velocity meter is capable to measure only one portion of the water surface, the instrument was traversed along the bridge to measure three locations

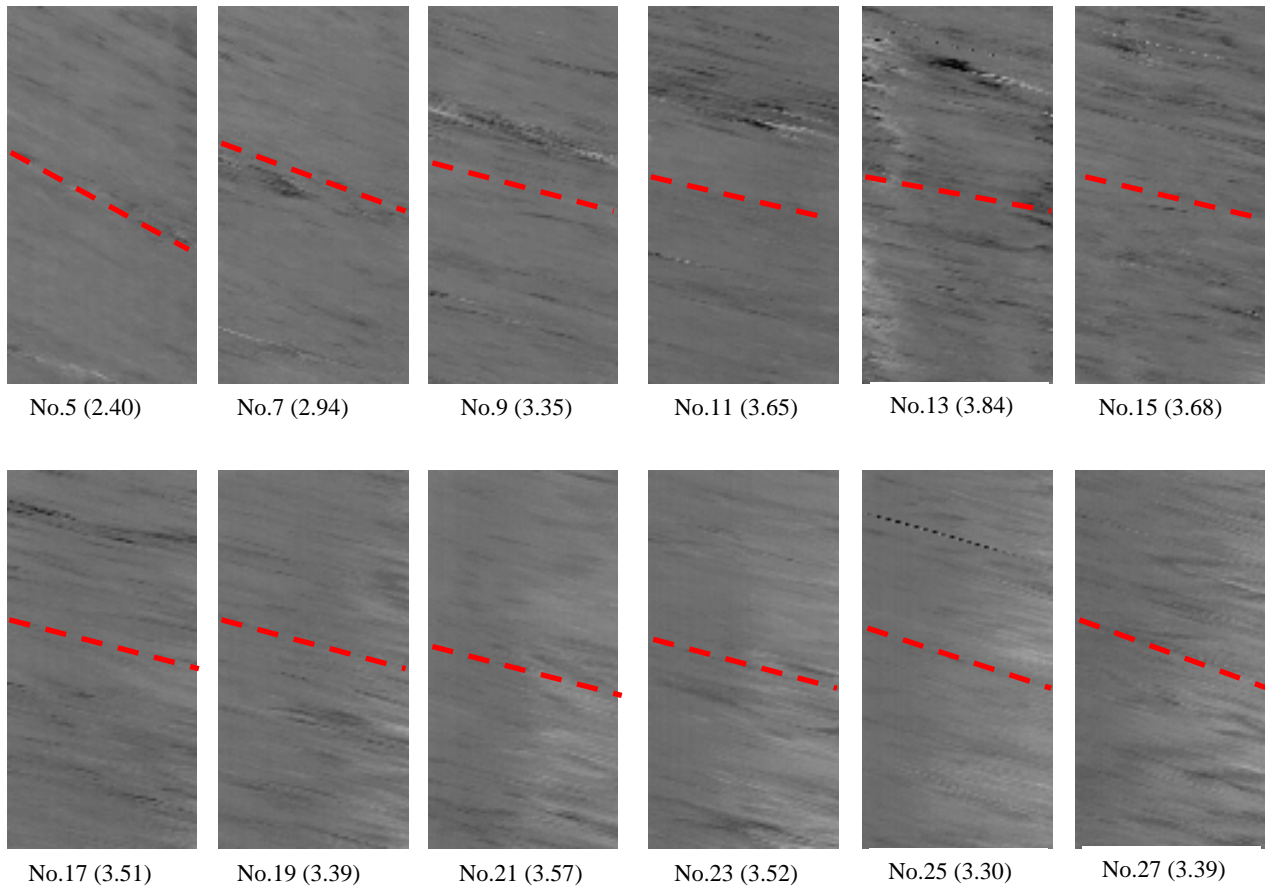


Fig.8 STIs from left bank video camera; horizontal scale is 10m and downward vertical scale is 20 seconds, the number in the bracket is velocity obtained by STIV, the starting time is 4:14:27 pm on Sept.3, 2011

that roughly covers the width of the river.

As an example, Fig.9 shows the comparison of velocity distributions measured by STIV and the radio-wave velocity meter. STIV results from the two video cameras agrees well with each other in most of the central regions. As previously mentioned, there exists an invisible water zone for each angle. Therefore, the velocity distributions obtained from the two angles successfully covered the entire water zone. The measurement of the whole zone at one shooting can be established if we can raise the video camera at a higher position and reduce the hidden zone by the nearest bank. It is important to note that the data at three locations measured by the radio-wave velocity meter fall into the velocity distribution obtained by STIV. This fact suggests that both methods are tracking the same physical phenomenon generated at the water surface. It is obvious the imaging technique yields much finer velocity distribution without any additional efforts than a radio-wave velocity meter. The other advantage of imaging technique is that it does not require a bridge for observation as in the case of the radio-wave velocity meter.

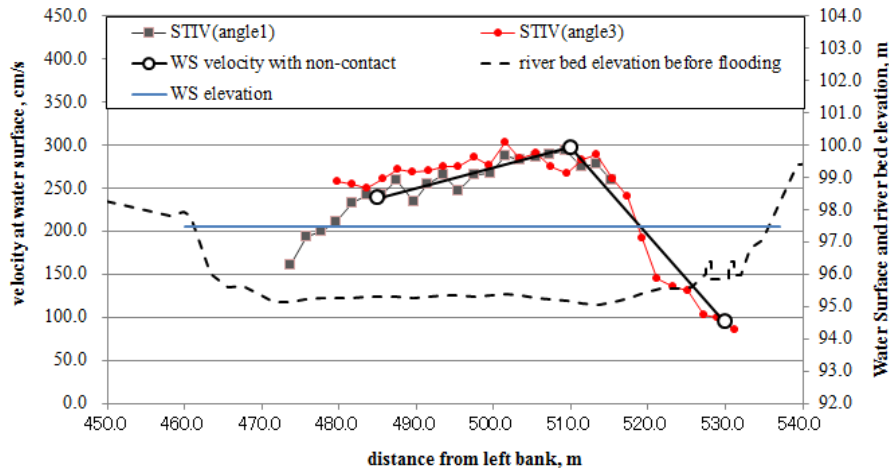


Fig.9 Comparison of surface velocity distributions; 11:53:23, Sept.2, 2011

CONCLUSIONS

Measurements of velocity distributions at a water surface during the relatively large Kinu River flood 2011 were conducted by an imaging technique and a radio-wave velocity meter. The features of space-time images used in the STIV measurements were explained in detail, e.g. in terms of the light reflection by the sun. From the fact that the velocity distributions measured from the two angles agreed fairly well, the water surface features based on the physical phenomenon was found to be independent of the viewing angle and seemed to be following the water surface flow. The additional evidence that the radio-wave velocity meter yielded data that fall into the distribution obtained by STIV, the traceability of water surface features was confirmed. Finally, it was shown that STIV is a reliable and efficient technique for flood flow measurements.

ACKNOWLEDGEMENTS

This research was supported by the Water and Disaster Management Bureau at the Ministry of Land, Infrastructure, Transport and Tourism. Their support by arranging the present project in all aspects is greatly appreciated.

REFERENCES

- Dinehart, R.L. and Burau, J. R. (2005), Averaged indicators of secondary flow in repeated acoustic Doppler current profiler crossings of bends, *Water Resources Research*, Vol.41, W09405(1-18).
- Fujita, I., and Komura, S. (1994), Application of video image analysis for measurements of river-surface flows, *Annual Journal of Hydraulic Engineering*, Japan Society of Civil Engineers, 38, pp.733-738 (in Japanese).
- Fujita, I., Aya, S. and Deguchi, T. (1997), Surface Velocity Measurement of River Flow Using Video Images of An Oblique Angle, *Proceedings of the 27th Congress of IAHR, Theme B*, Vol.1, San Francisco, CA, pp.227-232.
- Fujita, I., Muste, M. and Kruger, A. (1998), Large-scale particle image velocimetry for flow analysis in hydraulic engineering applications, *Journal of Hydraulic Research*, Vol.36, No.3, pp.397-414.
- Fujita, I., Watanabe, H. and Tsubaki, R. (2007), Development of a non-intrusive and efficient flow monitoring technique: The space time image velocimetry (STIV), *International Journal of River Basin Management*, 5(2), pp.105-114.
- Le Coz, J., G. Pierrefeu, and A. Paquier (2008), Evaluation of river discharges monitored by a fixed side-looking Doppler profiler, *Water Resources Research*, 44, W00D09, doi:10.1029/2008WR006967.



- Muste, M., K. Yu, and M. Spasojevic (2004), Practical aspects of ADCP data use for quantification of mean river flow characteristics; part I: Moving-vessel measurements, *Flow Meas. Instrument.*, 15(1), 1–16.
- Oberg, K. A., and D. S. Mueller (2007), Validation of streamflow measurements made with Acoustic Doppler Current Profilers, *J. Hydraul. Eng.*, 133(12), 1421–1432.
- Sun, X., Shiono, K., Chandler, J. H., Rameshwaran, P., Sellin, R.H.J. and Fujita, I. (2010), Discharge estimation in small irregular river using LSPIV, *Water Management*, 163 Issue WM5, pp.247-254.
- Teague, C. C., Barrick, D. E., Lilleboe, P. M., and Cheng, R.T. (2007), RiverSonde: measuring river surface velocity with UHF Radar, *Book of Extended Abstracts, Hydraulic Measurements & Experimental Methods*, pp.178-183.